31st Annual International Conference of the IEEE EMBS
Minneapolis, Minnesota, USA, September 2-6, 2009

Energy-Efficient Multihypothesis Activity-Detection for Health-Monitoring Applications

Gautam Thatte, Ming Li, Adar Emken, Urbashi Mitra,
Shri Narayanan, Murali Annavaram and Donna Spruijt-Metz

Abstract— **Multi-hypothesis activity-detection using a wireless body area network is considered. A fusion center receives samples of biometric signals from heterogeneous sensors. Due to the different discrimination capabilities of each sensor, an optimized allocation of samples per sensor results in lower energy consumption. Optimal sample allocation is determined by minimizing the probability of misclassification given the current activity state of the user. For a particular scenario, optimal allocation can achieve the same accuracy (97%) as equal allocation across sensors with an energy savings of 26%. As the number of samples is an integer, further energy reduction is achieved by developing an approximation to the probability of misclassification which allows for a continuous-valued vector optimization. This alternate optimization yields approximately optimal allocations with significantly lower complexity, facilitating real-time implementation.**

I. INTRODUCTION

Wireless body area networks (WBANs) are emerging as useful tools for continuous health monitoring. In this paper, we further develop the KNOWME network [1], a WBAN that is targeted to monitoring the movements of overweight children in an effort to gauge physical activity. We specifically consider the activity-detection problem [2]; using data from biometric sensors such as accelerometers and heart-rate monitors, our methods detect current participant behaviour – specific physical activity in which the participant is currently engaged, *e.g.* sitting, standing, or walking. There has been significant prior work on activity detection using on-body sensors; however much of the work uses accelerometers alone (*e.g.* [3], [4], [5]), or gyroscopes. More recent work [6], [7], [8] had used multiple heterogeneous sensors, focusing on higher layer communication network processing and hardware design. In contrast, we have developed signal processing strategies for activity-detection, and optimized the performance to increase energy-efficiency. We examine the efficacy of such methods in a "free-living" scenario in which subjects engage in activities of their own choosing.

Our KNOWME WBAN employs heterogeneous sensors in a star topology, which send samples to a cell phone fusion center via Bluetooth that employs a "serve as available" protocol. In this protocol, all samples taken by each sensor are collected by the fusion center. However, continuous functioning of Bluetooth requires undesirably high energy consumption, drastically reducing the battery life of the cellphone. Previous work on developing energy-efficient WBAN systems have used sleeping/waking cycles [9] and unused time redistribution [10], among many other techniques, to minimize energy consumption. Our work offers a new approach in that the energy-efficiency of the system is a result of optimized resource allocation; *i.e.* measurements are distributed among sensors according to which sensor is most informative in a given situation, rather than being equally distributed at all times. Our contributions are threefold: first, we develop a signaling/sampling protocol for free-living scenarios using a finite-state machine for transitions of activity (see *e.g.* [3]); second, we present an assessment of the energy-savings; last, we present the successful application of our sampling methods on real data.

This research is supported by the National Center on Minority Health and Health Disparities (supplement to P60 MD002254) and Qualcomm.

G. Thatte et al. are with the Ming Hsieh Department of Electrical Engineering, University of Southern California, Los Angeles, CA 90089

A. Emken and D. Spruijt-Metz are with the Keck School of Medicine, University of Southern California, Los Angeles, CA 90089

II. SYSTEM OVERVIEW

Our network currently employs a tri-axial accelerometer (ACC) and an electrocardiograph (ECG), both of which send samples to the cell phone fusion center. A *sample* is defined as an instance of a feature that is extracted from sensor data. In the case of the ECG, the feature extracted is the inter-peak period of the Electrocardiogram (ECG) waveform [11], and a sample represents one value of this period (see Figure 2). The ACC feature is the average of the acceleration signal variances in each axis for an ACC data segment, and a sample is the average variance of one such segment.

A system-level block diagram of the energy-efficient KNOWME network for activity-detection is shown in Figure 1. The *initialization stage* estimates model parameters for seven activities (Lying Down, Sitting, Standing, Sit&Fidget, Stand&Fidget, Walking and Running) for each test subject, using data from three separate structured activity periods. Data from a fourth, unstructured fee-living session is used to test the efficacy of our system, with the data divided into alternating training and optimization phases. During a training phase, the fusion center employs equal allocation for each sensor to detect the current activity/state. Knowledge of the current state and the probability of transition to the possible next states are used to derive the optimal allocation wherein only a subset of sensors are active; this is implemented in the optimized phase. The finite-state machine in Figure 3 is an exemplar of the state transition probabilities considered herein. Our previous work [12] considered the optimal allocation problem for the *static* case, *i.e.* it did not factor in the current state of the subject, but instead focused on the optimal allocation given a set of possible activities.

978-1-4244-3296-7/09/$25.00 ©2009 IEEE

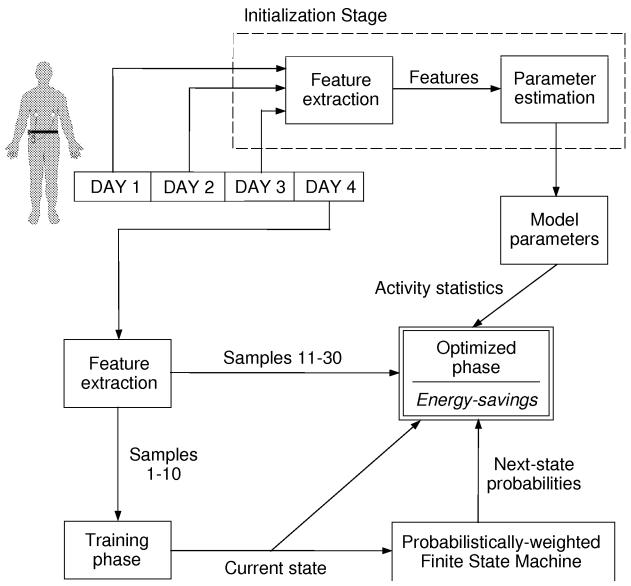

Fig. 1. System overview illustrating that the optimal allocation is a function of the current state, the next state probabilities, and the model parameters which are determined using structured activity data from three days. Unstructured activity data from a fourth day is used to test our algorithm wherein the training phase, using 10 out of 30 samples, determines the current state, and the remaining 20 out of 30 samples are optimized, resulting in energy-savings.

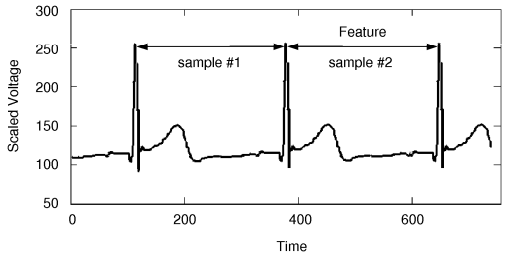

Fig. 2. Electrocardiograph (ECG) waveform showing the feature extracted – the ECG period – and a *sample* defined as one instance of the feature.

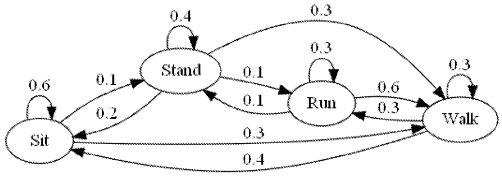

Fig. 3. Finite-state machine with nominal prior probabilities used for the optimal resource allocation case-study.

This work develops a framework through which to determine the evolution of optimal resource allocation as the subject transitions through different states.

III. PROBLEM FORMULATION

In this section, we present the signal model and outline our optimization problem: minimizing the probability of misclassification. As the number of samples N is an integer, optimal allocation requires an expensive combinatorial search. We thus develop an approximate metric based on a real-valued N, that yields an approximately optimal solution.

A. Signal Model

Biometric samples of the relevant features are sent by each of the heterogeneous sensors directly to the cell phone via Bluetooth. We make the following key assumptions. Based on our prior work [1], we approximate the statistics of the key features as Gaussian. To capture the temporal correlation of the features, we further impose an auto-regressive (AR), order 1 model. This model has been validated with our real biometric signals. The AR model has been previously employed to estimate electroencephalogram (EEG) signals [13] and physiological hand-tremors [14]. We allow for sensing and communication noise. For our selected features, the correlation between features (ACC and ECG) was found to be low [1], thus different sensor signals are modeled as uncorrelated[1]. This assumption is consistent with our observation that certain sensors better discriminate between some subsets of activities than others.

[1]Due to our jointly Gaussian feature model, lack of correlation implies statistical independence.

We now propose the following signal model for the decoded and processed samples received by the fusion center:

$$y_i = \theta_{jk} + z_i,\ i = 1, \ldots, N_k \tag{1}$$

for the k-th sensor and hypothesis H_j, where z_i represents the independent and identically distributed zero-mean Gaussian measurement and channel noise. For a feature A_k, θ is a normally distributed random variable, specified as

$$\theta_{jk} = \mu_{jA_k} + w_i \tag{2}$$

where w_i is modeled using the AR(1) model with parameter ϕ and variance $\sigma^2_{jA_k}$. To simplify notation, we omit the hypothesis subscript $_j$ when expressions and definitions are applied to a generic hypothesis. We denote the number of samples sent by the K sensors as $N_1, N_2, \ldots, N_K$, respectively, and impose the constraint $N = N_1 + N_2 + \cdots + N_K$, for a specific time-period.

The M-ary hypothesis test using the model in (1) is for the generalized Gaussian problem which is specified as

$$H_i: \quad \mathbf{Y} \sim N(\mathbf{m}_i, \mathbf{\Sigma}_i), \quad i = 1, \ldots, M, \tag{3}$$

where $\mathbf{m}_i, \mathbf{\Sigma}_i, i = 1, 2, \ldots, M$ are the mean vectors and covariance matrices of the observations under each of the hypotheses, and for the K-th feature A_k are of the form

$$\begin{aligned} \mathbf{m}_j &= \left[\mu_{jA_1}\ \mu_{jA_2}\ \cdots\ \mu_{jA_K}\right]^T \quad \text{and} \\ \mathbf{\Sigma}_j &= \text{diag}\left(\mathbf{\Sigma}_j(A_1), \mathbf{\Sigma}_j(A_2), \ldots, \mathbf{\Sigma}_j(A_K)\right), \end{aligned} \tag{4}$$

respectively. Note that μ_{jA_i} is a $N_i \times 1$ vector and $\mathbf{\Sigma}_j(A_i)$ is a $N_i \times N_i$ matrix. For a particular feature A_k, the covariance matrix can be expressed as

$$\mathbf{\Sigma}(A_k) = \frac{\sigma^2_{A_k}}{1-\varphi^2}\mathbf{T} + \sigma_z^2\mathbf{I}, \tag{5}$$

where $\mathbf{T}$ is a Toeplitz matrix whose first row/column is $[1\ \phi\ \phi^2\ \cdots\ \phi^{N_k-1}]$, and $\mathbf{I}$ is the $N_k \times N_k$ identity matrix. This results in the covariance matrices $\mathbf{\Sigma}_j, j = 1, \ldots, M$ being block-Toeplitz matrices.

B. Misclassification Metric Derivation

To optimize performance via sample allocation, we consider an upper bound on the probability of misclassification based on a union bound (sum of pair-wise errors). Extending our work in [12], which considered the static case, this analysis depends on the current state $\mathcal{S}$. We use the upper bound in [16]:

$$P(\epsilon|\mathcal{S}) \leq \sum_{i<j} \left(P_{i|\mathcal{S}} P_{j|\mathcal{S}}\right)^{1/2} \rho_{ij|\mathcal{S}}, \tag{6}$$

where $P_{i|\mathcal{S}}$ and $P_{j|\mathcal{S}}$ are the *a priori* probabilities for hypotheses H_i and H_j from the current state, and $\rho_{ij|\mathcal{S}}$ is the state-dependent Bhattacharyya coefficient given by:

$$\rho_{ij|\mathcal{S}} = \exp\left(-\frac{1}{8}\ m_d^T {\mathbf{\Sigma_h}}^{-1} m_d - \frac{1}{2}\ \ln \frac{|\mathbf{\Sigma}_h|}{\sqrt{|\mathbf{\Sigma}_i||\mathbf{\Sigma}_j|}}\right), \tag{7}$$

in the case of multivariate Gaussian hypotheses, where $m_d = m_i - m_j$, $|\mathbf{\Sigma}| = \det \mathbf{\Sigma}$, and $2\mathbf{\Sigma}_h = \mathbf{\Sigma}_i + \mathbf{\Sigma}_j$.

We first note that $\rho_{ij|\mathcal{S}}$ is a function of the means and covariances associated with the hypotheses H_i and H_j, and is a measure of the confusability of the two hypotheses. The upper bound incorporates classification errors that can be made between all **possible** pairs of hypotheses. Note that not all pairs are considered in the case of evolving activities undertaken by a subject. For example, as seen in Figure 3, if the subject is "Standing," then all three possible pairs of hypotheses are considered. In comparison, if the subject is "Sitting," the Sit→Run transition probability is 0, and so only two pairs of hypotheses are considered. Therefore, the optimal allocation depends on both the current state and the possible next state transition probabilities.

In order to derive the low-complexity implementation for the optimal allocation described above, we separately consider the quadratic and determinant terms in (7). Both the determinant and quadratic terms can be decomposed as a function of the individual features considered as follows:

$$\det \mathbf{\Sigma}_j \ = \ \prod_{k=1}^{K} \det \mathbf{\Sigma}_j(A_k), \tag{8}$$

$$\text{and} \quad \mu_d^T \mathbf{\Sigma}_h^{-1} \mu_d = \sum_{k=1}^{K} \mu_{dA_k}^T \mathbf{\Sigma}_h^{-1}(A_k) \mu_{dA_k}, \tag{9}$$

where $\mu_d = \mu_j - \mu_i$ and $\mu_{dA_k} = \mu_{jA_k} - \mu_{iA_k}$. Thus, computing each of the terms for an individual feature A_k is sufficient to evaluate the Bhattacharyya coefficient specified in (7).

To evaluate the determinant of $\mathbf{\Sigma}$, we use the Toeplitz structure of the covariance matrix, decompose the matrix into diagonal $\mathbf{\Sigma}_D$ and off-diagonal $\mathbf{\Sigma}_{\text{off}}$ pieces, and employ the identity [17]

$$\det \mathbf{\Sigma} = \det \mathbf{\Sigma}_D \cdot \det\left(\mathbf{I} + \mathbf{\Sigma}_D^{-1} \mathbf{\Sigma}_{\text{off}}\right), \tag{10}$$

in addition to the expansion of $\log(1+x)$ and the geometric progression to yield the required approximation. For the covariance matrix $\mathbf{\Sigma}(A_k)$ of a particular feature, the determinant term is evaluated as

$$\det \mathbf{\Sigma}(A_k) \ \approx \ \alpha^{N_k} e^{-C\left[-1+\phi^{2N_k}-N_k(1-\phi^{-2})\right]}, \tag{11}$$

where $\alpha = \sigma_{A_k}^2/(1-\phi^2) + \sigma_z^2$ and

$$C = 1/\alpha^2 (\sigma_{A_k}^2/(1-\phi^2))^2 \phi^{-2}/(1-\phi^{-2})^2$$

is a constant independent of N_k. The quadratic term is simplified using the circulant approximation[2] and a result by Wilansky [18] which exploits the fact that the sum of elements of a circulant matrix is constant for all rows. Then, applying a geometric progression identity results in the quadratic term in (7) for a particular feature A_k being simplified as

$$(\mu_{yA_k} - \mu_{xA_k})^2 N_k \left[\frac{\sigma_{yA_k}^2 (1-\phi^{N_k})}{(1-\phi^2)(1-\phi)} + \sigma_z^2\right]^{-1}, \tag{12}$$

for hypotheses H_i and H_j. The resulting expressions (11) and (12), which are fairly simple functions of N_k, may be evaluated for continuous values of N and the associated complexity is independent of the number of available samples N, *i.e.* $\mathcal{O}(1)$. In contrast, the combinatorial search is of order $\mathcal{O}(N^{K-1})$ given N samples and K sensors.

IV. NUMERICAL SIMULATIONS

In this section, we present a numerical analysis of the optimal allocation algorithm using experimental data collected from test subjects across four sessions as described in Section II. We note that our detection and optimal allocation methods require that the Gaussian model parameters be estimated individually for each test subject. Although the results a single subject are shown here, these results are representative of the remaining data set.

For clarity of exposition, we focus on the two-sensor case, the ACC and ECG, with four hypotheses (Sitting, Standing, Walking and Running), and note that our methods are directly applicable to multiple sensors [19]. The ACC variance and the ECG period are allocated N_1 and N_2 samples, respectively. The distributions associated with each of the hypotheses for these two features for a single participant are shown in Figure 4. Note that the Bhattacharyya exponents measure the "distance" between two distributions.

We evaluate our energy-efficient activity-detection mechanism using a 522-sample (approximately 20 minute) free-living scenario. Figure 5 shows the testing scenario – the subject activities, the decisions taken by the detector, and the evolution of the optimal allocation, for the case wherein 10 of every 30 samples are used for training. In particular, the third subplot (% ACC) shows the optimal allocation of

[2]We note that the inverse of the Toeplitz covariance matrix in (5) converges to the inverse of the circulant covariance matrix in the weak sense as N grows large. A sufficient condition for weak convergence [15] is met for our matrix forms for $0 < \phi < 1$.

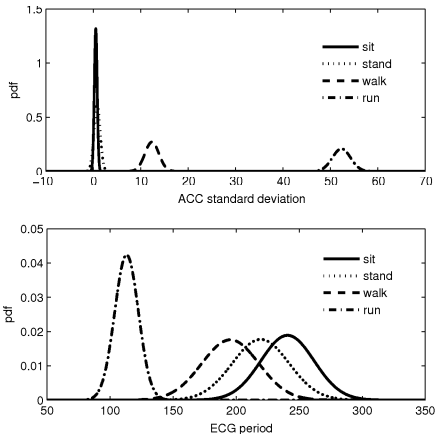

Fig. 4. Gaussian distributions associated with each of the four activities for the ACC StdDev and ECG period features. The upper plot clearly indicates that the ACC StdDev is not a good discriminator between the Sit and Stand activities, but the ECG period is, as evidenced in the lower plot.

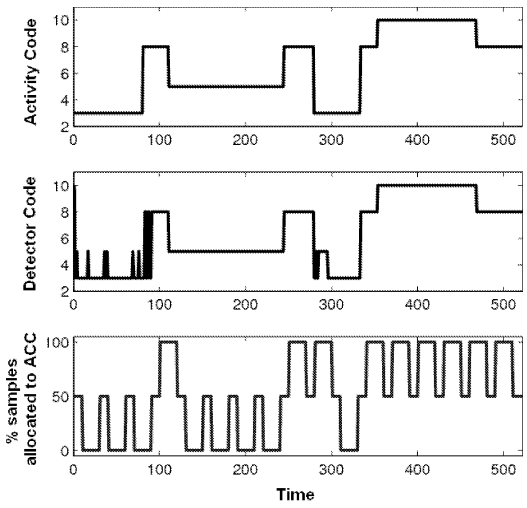

Fig. 5. The optimal allocation algorithm applied to the free-living testing scenario: subplots 1 and 2 show subject activities (3=Sit, 5=Stand, 8=Walk, 10=Run) and detector decisions, respectively. Subplot 3 shows the optimal allocation of ACC samples. We note that 50% ACC corresponds to the training phase, and that the ACC is allocated all samples when the subject is engaged in the high-level activities, i.e. Walking and Running.

samples to the accelerometer. We note that allocation is time-varying and depends on the current state of the subject, and that the time during which 50% of the samples allocated to the ACC period corresponds to the training phase of our algorithm. Table I shows the detection accuracy achieved for different training periods. We find that more training, and more frequent training, is preferred.

We use the following algorithm to quantify the energy-savings associated with using only one sensor: given the probability of error for the optimal allocation of N samples, we compute the minimum number of equally allocated samples that would have been required to achieve the same probability of error. Given that each sensor is better at detecting a particular state, if we match states to the appropriate sensor, using only ACC or ECG samples results in energy-savings of 43% and 46%, respectively. Thus, we find that as an alternative to 97% accuracy using samples from all sensors, our optimal sampling method also achieves 97% detection accuracy with approximately 26% energy-savings.

TABLE I
DETECTION ACCURACY FOR DIFFERENT TRAINING SCENARIOS.

Training frequency	10 of 50	25 of 125	10 of 30	25 of 75
Detection accuracy	90.2%	90.4%	97%	92.3%

V. CONCLUSIONS

An energy-efficient and low-complexity mechanism for free-living activity-detection is developed in this work. We consider activity transitions, and find that unequally allocating samples amongst sensors yields better performance, or energy-savings, compared to equally allocating samples. Our algorithm is tested on real data to show that optimal allocation provides noticeable energy-savings as compared to activating all sensors equally. The continuous-valued vector optimization derived is significantly lower complexity than a combinatorial search.

REFERENCES

[1] M. Annavaram et al. Multimodal sensing for pediatric obesity applications. In *Proceedings of UrbanSense08*, Raleigh, NC, Nov 2008.
[2] D. Spruijt-Metz et al. Differentiating physical activity modalities in youth using heartbeat waveform shape and differences between adjacent waveforms. *7th ICDAM*, Washington DC, June 2009.
[3] S. Biswas and M. Quwaider. Body posture identification using HMM with wearable sensor networks. In *Proc. of BodyNets*, March 2008.
[4] S. Jiang et al. Carenet: An integrated wireless sensor networking environment for remote healthcare. In *Proc. of BodyNets*, March 2008.
[5] A. Kalpaxis. Wireless temporal-spatial human mobility analysis using real-time three dimensional acceleration data. In *Proc. of Intl. Multi-Conference on Computing in Global Info. Technology*, March 2007.
[6] F. Dabiri, H. Noshadi, H. Hagopian, et al. Light-weight medical bodynets. In *Proc. of BodyNets*, Florence, Italy, June 2007.
[7] E. Jovanov et al. A wireless body area network of intelligent motion sensors for computer assisted physical rehabilitation. *Journal of NeuroEngineering and Rehabilitation*, 2:6, March 2005.
[8] S. Consolvo et al. Activity sensing in the wild: A field trial of Ubifit garden. In *Conf. on Human Factors in Computing Systems*, 2008.
[9] A. Benbasat and J. Paradiso. Framework for the automated generation of power-efficient classifiers for embedded sensor nodes. In *Proc. of SenSys*, Sydney, Australia, Nov 2007.
[10] Y. Liu et al. Critical-path based low-energy scheduling algorithms for body area network systems. In *Proc. of RTCSA*, Korea, Aug 2007.
[11] D. A. Warrell et al. *Oxford Textbook of Medicine.* OUP, 2005.
[12] G. Thatte et al. Optimal Time-Resource Allocation for Activity-Detection via Multimodal Sensing. In *Proc. of BodyNets*, April 2009.
[13] G. Mohammadi et al. Person identification by using AR model for EEG signals. *Proceedings of the World Academy of Science, Engineering and Technology*, Vol. 11, Feb 2006.
[14] J. Zhang and F. Chu. Real-time modeling and prediction of physiological hand tremor. In *Proc. of ICASSP*, Philadelphia, PA, Mar 2005.
[15] F.-W. Sun et al. On the convergence of the inverses of Toeplitz matrices and its applications. *IEEE Trans IT*, 49(1), January 2003.
[16] D. Lianiotis. A class of upper bounds on probability of error for multihypotheses pattern recognition. *IEEE Trans IT*, Nov 1969.
[17] I. Ipsen and D. Lee. Determinant approximations. *Numerical Linear Algebra with Applications*, (Under review), 2006.
[18] A. Wilansky. The row-sums of the inverse matrix. *The American Mathematical Monthly*, 58(9):614615, November 1951.
[19] G. Thatte et al. Optimal Allocation of Time-Resources for Multihypothesis Activity-Level Detection. In *Proc. of DCOSS*, Marina Del Rey, CA, June 2009.